11th International Symposium on Turbulence and Shear Flow Phenomena (TSFP11)
Southampton, UK, July 30 to August 2, 2019

TWO-SCALE INTERACTION IN NEAR-WALL TURBULENCE

Patrick Doohan
Department of Aeronautics
Imperial College London
London SW7 2AZ, United Kingdom
patrick.doohan15@imperial.ac.uk

Elena Marensi
School of Mathematics and Statistics
University of Sheffield
Sheffield S3 7RH, United Kingdom
e.marensi@sheffield.ac.uk

Ashley P. Willis
School of Mathematics and Statistics
University of Sheffield
Sheffield S3 7RH, United Kingdom
a.p.willis@sheffield.ac.uk

Yongyun Hwang
Department of Aeronautics
Imperial College London
London SW7 2AZ, United Kingdom
y.hwang@imperial.ac.uk

ABSTRACT

The temporal dynamics of a two-scale near-wall flow are investigated, with a particular emphasis on nonlinear turbulent transport between the scales. The energy balance equations at each scale are derived, and their statistics and dynamics are analysed. The temporal dynamics of the energy-containing eddies at each scale follow the self-sustaining process, based on the interaction between streaks and quasi-streamwise vortices. It is shown that the turbulent production term correlates well with the lift-up effect and the pressure transport term correlates well with streak instability, at both large and small scales. Across the wall-normal domain, the dominant scale interaction process is the cascade of energy from large to small scales and it is most active during the late stages of streak breakdown. However, very close to the wall, energy transfer from small to large scales occurs highly intermittently and it leads to the formation of large-scale wall-parallel velocity structures. In the presentation, the full dynamics of the two-scale interaction system will be discussed in detail.

INTRODUCTION

There is a growing body of evidence indicating that wall-bounded turbulence is comprised of a hierarchy of energy-containing eddies, as described by Townsend (1980) in the attached-eddy hypothesis. Townsend postulated that the characteristic lengthscale of these eddies is approximately proportional to the distance from the wall, with the smallest eddies being located in the near-wall region and scaling in inner units, and the largest eddies occupying the entire wall-normal domain and scaling in outer units. Furthermore, it was hypothesised that these coherent structures were statistically self-similar with respect to the given lengthscale. Several recent studies have supported Townsend's theory, including the linear growth of the spanwise integral lengthscale with distance from the wall (Tomkins & Adrian, 2003), the logarithmic dependence of the turbulence intensities of wall-parallel velocity components (Marusic *et al.*, 2013) and the self-similarity of structures of various spanwise lengthscales in the logarithmic layer (Hwang, 2015). It has also been shown that the sustainment of energy-containing structures of a particular lengthscale in the hierarchy occurs even in the absence of motion at other scales, including in the near-wall region (Jiménez & Pinelli, 1999), the logarithmic layer (Hwang & Cossu, 2011) and the wake layer (Hwang & Cossu, 2010). In particular, the temporal dynamics of isolated energy-containing eddies at each scale are remarkably similar to the self-sustaining process of the near-wall region (Hwang & Bengana, 2016), based on the interaction between streaks and quasi-streamwise vortices (Hamilton *et al.*, 1995).

However, the existence of this scale-independent self-sustaining process does not imply that the interaction between structures of different scales in the hierarchy is unimportant. To the contrary, the key process of turbulent dissipation is the Richardson-Kolmogorov energy cascade (Kolmogorov, 1941, 1991), in which turbulent kinetic energy is produced at the integral lengthscale, transported down to the smallest possible lengthscale and dissipated into heat by the fluid viscosity. Such scale interaction processes appear to be crucial in the near-wall region, to which coherent structures of all scales in the hierarchy would contribute. For example, it has been demonstrated that the interaction between wall-attached structures of different scales plays a key role in skin-friction generation (de Giovanetti *et al.*, 2016). In addition, it appears that scale interaction is responsible for the inner-scaling of coherent structures in the near-wall region itself (Hwang, 2016).

Several previous studies have explored scale interaction in the near-wall region, specifically between the self-sustaining inner structures and near-wall penetrating outer structures (e.g. Mathis *et al.*, 2009; Agostini & Leschziner, 2016). The most commonly used technique in such analyses is a decomposition of the near-wall velocity field into inner and outer components, so as to understand the superposition/modulation effect of the outer structures on the near-wall dynamics. However, such a binary decomposition is incompatible with the attached eddy hypothesis, which asserts that the near-wall velocity field is influenced by coherent structures of all scales in the hierarchy. To reconcile the study of scale interaction with the attached eddy hypothe-

sis, Cho *et al.* (2018) considered the equation of the turbulent kinetic energy of each spanwise Fourier mode, which adequately characterises the size of the coherent structures (Hwang, 2015). Through the visualisation of the triad wave interactions of the nonlinear turbulent transport term, this work confirmed the role of the classical energy cascade and identified two new scale interaction processes; the involvement of larger structures in the energy cascade of smaller structures and the non-negligible energy transfer from small to large scales in the near-wall region.

Despite this important progress in statistically steady turbulence, the temporal dynamics of flows with multiple scales of motion are not well understood and this is the issue that this work seeks to address. For this purpose, the ideal flow configuration is the shear stress-driven model (Doohan *et al.*, 2019), which has been introduced recently. This model describes the dynamics of the inner-scaling (universal) part of near-wall turbulence in the absence of outer flow, as the friction Reynolds number $Re_\tau \to \infty$. The key feature of the shear stress-driven model is that it is applicable to the near-wall region and lower logarithmic layer of turbulent Couette, Poiseuille and Hagen-Poiseuille flow, since as $Re_\tau \to \infty$, the effects of the flow geometry or curvature are not felt. Therefore, the model allows for the most general analysis of multiscale turbulence near the wall. In this study, shear stress-driven flow in a domain just large enough to sustain two integral lengthscales of motion is considered. The velocity field is decomposed into large- and small-scale components, and the momentum and energy balance equations at each scale are derived. The statistics and dynamics of the nonlinear turbulent transport terms are analysed, and related to scale interaction processes.

NUMERICAL METHODS

Shear Stress-Driven Model

The flow considered is that of incompressible fluid in a rectangular domain, as described by the shear stress-driven model of Doohan *et al.* (2019). The model is formulated in inner units, with domain dimensions (L_x^+, L_y^+, L_z^+), spatial co-ordinates $\mathbf{x}^+ = (x^+, y^+, z^+)$ and velocity components $\mathbf{u}^+ = (u^+, v^+, w^+)$. Employing the Reynolds decomposition, the velocity field can be expressed in terms of the mean and fluctuating velocity components $\mathbf{u}^+(\mathbf{x}^+, t^+) = \mathbf{U}^+(y^+, t^+) + \mathbf{u}'^+(\mathbf{x}^+, t^+)$, which satisfy the equations

$$\frac{d\overline{U}^+}{dy^+} - \overline{\langle u'^+ v'^+ \rangle}_{x^+,z^+} = 1 \tag{1}$$

and

$$\begin{aligned} &\mathbf{u}_{t^+}'^+ + (\mathbf{U}^+ \cdot \nabla)\mathbf{u}'^+ + (\mathbf{u}'^+ \cdot \nabla)\mathbf{U}^+ = -\nabla p'^+ \\ &+ \nabla^2 \mathbf{u}'^+ - \left((\mathbf{u}'^+ \cdot \nabla)\mathbf{u}'^+ - \langle (\mathbf{u}'^+ \cdot \nabla)\mathbf{u}'^+ \rangle_{x^+,z^+} \right) \end{aligned} \tag{2}$$

respectively, where p'^+ is the pressure fluctuation, $\langle \cdot \rangle_{x^+,z^+}$ denotes the average in the streamwise and spanwise directions, and $\overline{\cdot}$ denotes the average in time. The layer of fluid above the wall that scales in inner units is called the mesolayer (e.g. Wei *et al.*, 2005), which has been observed in the mean-momentum equation. The extent of the mesolayer scales with the wall-normal location of maximum Reynolds stress as $y^+_{max} \sim \sqrt{Re_\tau}$ (Long & Chen, 1981; Sreenivasan & Sahay, 1997), since the viscous wall effects are non-negligible below this point. Therefore, within the mesolayer, the $-y^+/Re_\tau$ term derived from any imposed pressure gradient will vanish as $Re_\tau \to \infty$ and the right hand side of equation (1) above is just unity. Furthermore, the extent of the mesolayer increases as Re_τ increases and in the high-Re_τ limit, the mesolayer encompasses a hierarchy of scales. Hence, arbitrary values of the domain dimensions can be fixed, under the assumption that $L_x^+, L_y^+, L_z^+ \ll \sqrt{Re_\tau}$.

At the lower boundary of the domain, the no-slip condition $\mathbf{u}^+\big|_{y^+=0} = \mathbf{0}$ is imposed to represent the stationary wall. At the upper boundary, a horizontally-uniform shear stress is applied such that the bulk flow rate across the domain is maintained during simulations. The streamwise boundary condition is expressed as

$$\begin{aligned} u^+_{y^+}\Big|_{y^+=L_y^+}(t^+) = &\left\langle u^+_{y^+}\Big|_{y^+=0} \right\rangle_{x^+,z^+}(t^+) \\ &+ C^+(U_0^+ - U_b^+(t^+)) \end{aligned} \tag{3}$$

where $U_b^+(t^+)$ is the instantaneous bulk velocity, U_0^+ is the laminar bulk velocity and C^+ is a constant that maintains $U_b^+(t^+)$ close to U_0^+. This technique is very similar to that used to maintain constant mass flux in pressure-driven channel flow. Impermeability and stress-free conditions are imposed at the upper boundary for the wall-normal and spanwise components respectively, namely $v^+\big|_{y^+=L_y^+} = 0$ and $w^+_{y^+}\big|_{y^+=L_y^+} = 0$. Taking the time-average of equation (3) and given the impermeability condition, the mean-momentum equation (1) is indeed satisfied at the upper boundary of the domain. Periodic boundary conditions are imposed in both the streamwise and spanwise directions. Further details about the model and its validation are discussed in Doohan *et al.* (2019).

Given its formulation in inner units, the shear stress-driven model is governed by the unit-Reynolds number Navier-Stokes equations (2) and the inner-scaled domain dimensions (L_x^+, L_y^+, L_z^+) take on the role of control parameters. In particular, due to the periodic boundary conditions in the streamwise and spanwise directions, the domain size can be used to determine the expected hierarchy of integral lengthscales of motion. As a first step in the study of the temporal dynamics of multiscale mesolayer turbulence, the number of integral lengthscales is restricted to two. To this end, the domain size is fixed at $(L_x^+ = 640, L_y^+ = 180, L_z^+ = 220)$, hence only eddy-containing eddies with spanwise lengthscales $\lambda_z^+ \approx 220$ and $\lambda_z^+ \approx 110$ will be resolved (Jiménez & Moin, 1991), and structures of larger lengthscales will be removed. In this way, the model allows for the simplest analysis of the dynamics of a two-scale interaction system.

Two-Scale Governing Equations

In order to represent the motions at each integral lengthscale, the fluctuating velocity component is decomposed as $\mathbf{u}'^+ = \mathbf{u}_l^+ + \mathbf{u}_s^+$, where $\mathbf{u}_l^+$ and $\mathbf{u}_s^+$ denote the large- and small-scale structures respectively. As of now, no assumption is made as to the definition of $\mathbf{u}_l^+$ and $\mathbf{u}_s^+$ other than that they are disjoint sets. Substitution of $\mathbf{u}_l^+$ and $\mathbf{u}_s^+$ into (2) yields the large- and small-scale momentum equa-

tions

$$\frac{\partial \mathbf{u}_l^+}{\partial t^+} + (\mathbf{U}^+ \cdot \nabla)\mathbf{u}_l^+ = -(\mathbf{u}_l^+ \cdot \nabla)\mathbf{U}^+ - \nabla p_l^+ + \nabla^2 \mathbf{u}_l^+ - \mathscr{P}_l\{ (\mathbf{u}_l^+ \cdot \nabla)\mathbf{u}_l^+ + (\mathbf{u}_l^+ \cdot \nabla)\mathbf{u}_s^+ + (\mathbf{u}_s^+ \cdot \nabla)\mathbf{u}_l^+ + (\mathbf{u}_s^+ \cdot \nabla)\mathbf{u}_s^+ \} \tag{4}$$

and

$$\frac{\partial \mathbf{u}_s^+}{\partial t^+} + (\mathbf{U}^+ \cdot \nabla)\mathbf{u}_s^+ = -(\mathbf{u}_s^+ \cdot \nabla)\mathbf{U}^+ - \nabla p_s^+ + \nabla^2 \mathbf{u}_s^+ - \mathscr{P}_s\{ (\mathbf{u}_s^+ \cdot \nabla)\mathbf{u}_s^+ + (\mathbf{u}_s^+ \cdot \nabla)\mathbf{u}_l^+ + (\mathbf{u}_l^+ \cdot \nabla)\mathbf{u}_s^+ + (\mathbf{u}_l^+ \cdot \nabla)\mathbf{u}_l^+ \} \tag{5}$$

where $p'^+ = p_l^+ + p_s^+$ are the large- and small-scale pressure fluctuations, and $\mathscr{P}_l\{\ \cdot\ \}$ and $\mathscr{P}_s\{\ \cdot\ \}$ denote projection onto large- and small-scales respectively. Here, it should be noted that all of the terms in equations (4) and (5) are linear except for the advection terms, through which all scale interaction occurs.

Multiplying equation (4) by $\mathbf{u}_l^+$ and averaging in the streamwise and spanwise directions yields the large-scale energy balance equation, which can be written in component form as

$$\begin{aligned} \frac{\partial E_{ul}^+}{\partial t^+} &= P_{ul}^+ + T_{ul}^+ + T_{p,ul}^+ + T_{\nu,ul}^+ - \varepsilon_{ul}^+ \\ \frac{\partial E_{vl}^+}{\partial t^+} &= \qquad T_{vl}^+ + T_{p,vl}^+ + T_{\nu,vl}^+ - \varepsilon_{vl}^+ \\ \frac{\partial E_{wl}^+}{\partial t^+} &= P_{wl}^+ + T_{wl}^+ + T_{p,wl}^+ + T_{\nu,wl}^+ - \varepsilon_{wl}^+ \end{aligned} \tag{6}$$

where $E_{ul}^+ = \frac{1}{2}\langle u_l^{+2}\rangle$ is the kinetic energy, $P_{ul}^+ = -U_{y^+}^+ \langle u_l^+ v_l^+\rangle$ is the turbulent production, $T_{ul}^+ = -\langle u_l^+ (\mathbf{u}_l^+ \cdot \nabla u_l^+ + \mathbf{u}_l^+ \cdot \nabla u_s^+ + \mathbf{u}_s^+ \cdot \nabla u_l^+ + \mathbf{u}_s^+ \cdot \nabla u_s^+)\rangle$ is the turbulent transport, $T_{p,ul}^+ = -\langle u_l^+ p_{l_x^+}^+\rangle$ is the pressure transport, $T_{\nu,ul}^+ = \frac{1}{2}\langle u_l^{+2}\rangle_{y^+y^+}$ is the viscous transport and $\varepsilon_{ul}^+ = \langle (u_{l_x^+}^+)^2 + (u_{l_y^+}^+)^2 + (u_{l_z^+}^+)^2\rangle$ is the dissipation of the large-scale streamwise component. Analogous definitions exist for the terms in the small-scale streamwise energy-balance equation, namely E_{us}^+, P_{us}^+, T_{us}^+, $T_{p,us}^+$, $T_{\nu,us}^+$ and ε_{us}^+, as well as for the large- and small-scale wall-normal and spanwise equations.

The turbulent transport terms can be further decomposed into same-scale and inter-scale transport i.e. $T_{ul}^+ = T_{ss,ul}^+ + T_{in,ul}^+$, where the same-scale term only depends on the velocity components at that scale (e.g. $T_{ss,ul}^+ = -\langle u_l^+ (\mathbf{u}_l^+ \cdot \nabla u_l^+)\rangle$) and the inter-scale term depends on both large- and small-scale velocity components. All of the terms in the energy balance equations represent same-scale processes (e.g. pressure transport, dissipation etc.) apart from the inter-scale transport terms, hence any scale interaction process must be linked to these functions. Furthermore, the inter-scale turbulent transport terms for each component can be re-written such that the negation of the same term appears in the large- and small-scale energy balance equations for that component

$$\begin{aligned} T_{ul}^+ &= T_{ss,ul}^+ + T_{in,ul}^{+*} - T_{uls}^+ \\ T_{us}^+ &= T_{ss,us}^+ + T_{in,us}^{+*} + T_{uls}^+ \end{aligned} \tag{7}$$

hence it represents same-component inter-scale turbulent transport, i.e. the direct transfer of energy from e.g. u_l^+ to u_s^+. The terms in the energy-balance equations described above are the observables used to study the temporal dynamics of two-scale near wall turbulence.

MEAN TURBULENT STATE

Having introduced the shear stress-driven model and the energy balance equations at each scale, the task at hand is to analyse the temporal dynamics of the two-scale system. Before this can be done however, the statistics and spectra of the mean turbulent state must first be analysed in order to identify the scale-interaction processes of interest.

Spectra

The premultiplied streamwise turbulent transport (T_u^+) co-spectra of the mean turbulent state is shown in figure 1, as a function of the wall-normal height y^+ and the spanwise wavelength λ_z^+. The turbulent transport shows regions of both energy gain (red) and energy loss (blue). The negative values of T_u^+ correspond to the regions where the turbulent production (P_u^+) is active, representing the energy-containing eddies at both scales. For $\lambda_z^+ \approx 200$, the negative values of T_u^+ extend across the entire wall-normal domain, whereas for $\lambda_z^+ \approx 100$, the negative values only reach $y^+ \approx 50$. For each $y^+ > 10$, positive values of T_u^+ are found at smaller wavelengths than those of the negative values, corresponding to the regions where dissipation (ε_u^+) is dominant. This indicates that there is energy transfer from larger- to smaller-scales i.e. energy cascade, reaffirming the classical role of the turbulent transport term. However, there is also a region of positive T_u^+ very close to the wall ($y^+ < 15$), which has been identified in previous studies (e.g. Lee & Moser, 2015; Cho *et al.*, 2018). In particular, Cho *et al.* (2018) showed that this was the manifestation of energy transfer from smaller- to larger-scales and it is apparent from figure 1 that the value of T_u^+ in this region increases as λ_z^+ increases.

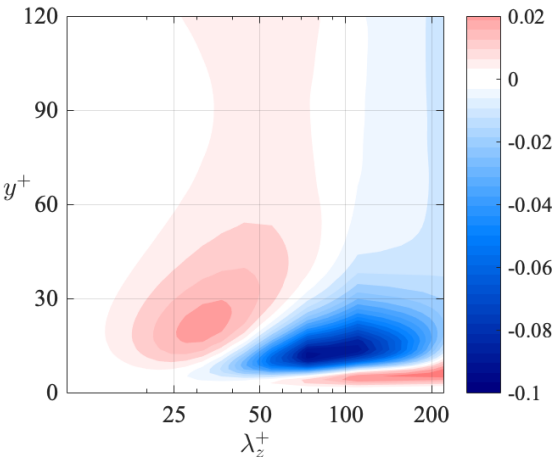

Figure 1. Premultiplied one-dimensional spanwise wavelength co-spectra of streamwise turbulent transport T_u^+.

It must be pointed out that the large- and small-scale velocity components have not yet been formally defined. In

accordance with the spectra above, $\mathbf{u}_l^+$ and $\mathbf{u}_s^+$ are hereby defined as

$$\begin{aligned}\mathbf{u}_l^+ &= \sum_{m=-1}^{1}\sum_{n=-1}^{1} \widehat{\mathbf{u}'^+} e^{i(mk_x x^+ + nk_z z^+)}, |m|+|n| \neq 0 \\ \mathbf{u}_s^+ &= \mathbf{u}'^+ - \mathbf{u}_l^+\end{aligned} \tag{8}$$

where $\widehat{\cdot}$ denotes the Fourier transform, and k_x and k_z are the fundamental streamwise and spanwise wavenumbers. Defining variables that represent the motions at each integral lengthscale then allows for the analysis of the statistics and temporal dynamics of the scale interaction processes described above.

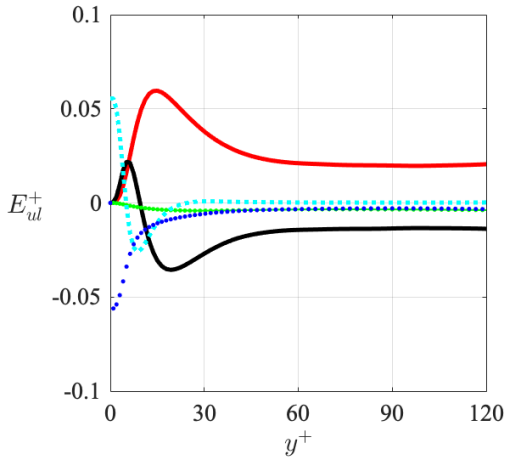

Figure 2. Energy balance of u_l^+: P_{ul}^+ (red), T_{ul}^+ (black), $T_{p,ul}^+$ (green), $T_{\nu,ul}^+$ (cyan) and $-\varepsilon_{ul}^+$ (blue).

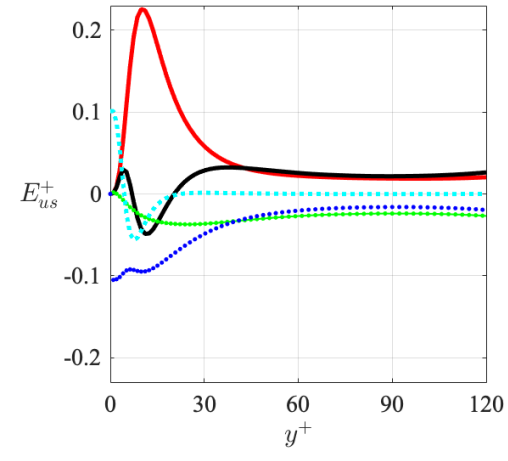

Figure 3. Energy balance of u_s^+: P_{us}^+ (red), T_{us}^+ (black), $T_{p,us}^+$ (green), $T_{\nu,us}^+$ (cyan) and $-\varepsilon_{us}^+$ (blue).

Statistics

The terms in the u_l^+ and u_s^+ energy balance equations, as a function of the wall-normal height y^+, are shown in figures 2 and 3 respectively. It is immediately obvious that the energy balance of the large-scale structures is primarily between production and negative turbulent transport, whereas that of the small-scale structures is primarily between production and positive turbulent transport, and dissipation. For $y^+ > 50$, the terms in the energy balance equations appear almost isotropic with little change with y^+, whereas the statistics are highly anisotropic closer to the wall. In particular, the turbulent transport terms T_{ul}^+ and T_{us}^+ are highly dependent on the wall-normal height. The wall-normal position of minimum T_{ul}^+ and T_{us}^+ coincides with the wall-normal position of maximum P_{ul}^+ and P_{us}^+, indicating where the energy-containing motions at each scale are most active. T_{ul}^+ achieves its maximum value in a peak close to the wall, corresponding to the region of positive turbulent transport in figure 1. T_{us}^+ has a similar peak but over a noticeably smaller interval in y^+.

TEMPORAL DYNAMICS

Following the analysis of the mean turbulent state in the previous section, the terms in the energy balance equations (6) are now integrated across the wall-normal domain and the temporal dynamics of the two-scale interaction system are investigated.

Self-Sustaining Processes

Firstly, the temporal dynamics of the energy-containing motions at each scale must be analysed. For this purpose, the velocity components are decomposed into their x^+-independent and -dependent parts, and the kinetic energies of large-scale 'straight' and 'wavy' streaks and rolls are defined as

$$\begin{aligned}E_{ss,l}^+(t^+) &= \frac{1}{2}\langle\langle u_l^+\rangle_{x^+}^2\rangle_{y^+,z^+} \\ E_{ws,l}^+(t^+) &= \frac{1}{2}\langle(u_l^+ - \langle u_l^+\rangle_{x^+})^2\rangle_{x^+,y^+,z^+} \\ E_{sr,l}^+(t^+) &= \frac{1}{2}\langle\langle v_l^+\rangle_{x^+}^2 + \langle w_l^+\rangle_{x^+}^2\rangle_{y^+,z^+} \\ E_{wr,l}^+(t^+) &= \frac{1}{2}\langle(v_l^+ - \langle v_l^+\rangle_{x^+})^2 + (w_l^+ - \langle w_l^+\rangle_{x^+})^2\rangle_{x^+,y^+,z^+}\end{aligned} \tag{9}$$

with equivalent definitions for the small-scale counterparts. Temporal cross-correlations indicate that the above observables occur in the order $E_{sr}^+ \rightarrow E_{ss}^+ \rightarrow E_{ws}^+ \rightarrow E_{wr}^+$ at both large- and small-scales, consistent with the self-sustaining process (Hamilton *et al.*, 1995).

The turbulent production terms P_{ul}^+ and P_{us}^+, which represent turbulent transport by the mean, fuel the self-sustaining process at each scale. In order to analyse the dynamics of this interaction, the temporal cross-correlations of production and the self-sustaining process are analysed. The cross-correlations of P_{ul}^+ and $E_{ss,l}^+$ at large-scale, and P_{us}^+ and $E_{ss,s}^+$ at small-scale are shown in red in figures 4 and 5. It is apparent that turbulent production correlates well with the energy of 'straight' streaks at both scales. The peaks are shifted slightly to the left, indicating that production fluctuates in line with the lift-up effect, which is responsible for the amplification of the streaks. Given that energy is only pumped into the streamwise velocity component, it must is redistributed to the wall-normal and spanwise components and this mainly occurs through the pressure transport

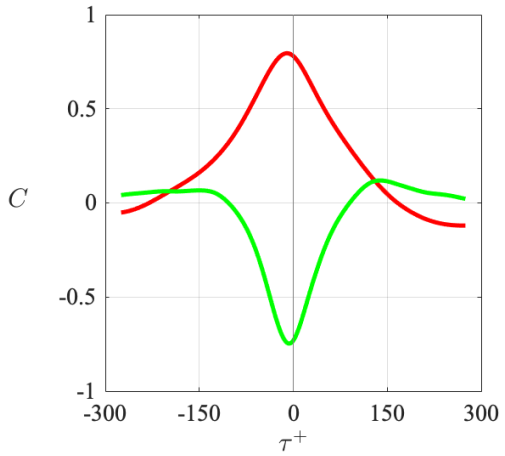

Figure 4. Temporal cross-correlations between P^+_{ul} & $E^+_{ss,l}$ (red), and $T^+_{p,ul}$ & $E^+_{ws,l}$ (green).

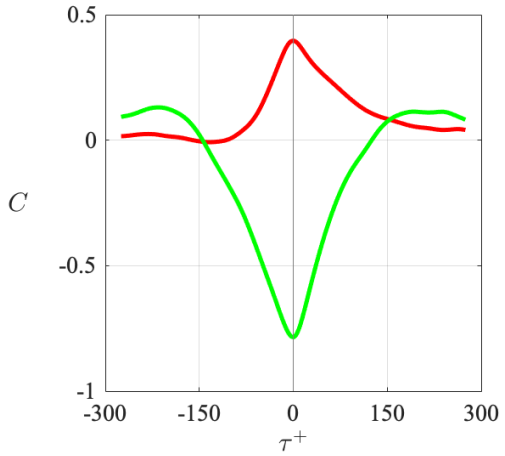

Figure 5. Temporal cross-correlations between P^+_{us} & $E^+_{ss,s}$ (red), and $T^+_{p,us}$ & $E^+_{ws,s}$ (green).

term. Again, the precise timing of this redistribution is investigated through cross-correlation with the self-sustaining process. The cross-correlations of $T^+_{p,ul}$ and $E^+_{ws,l}$ at large-scale, and $T^+_{p,us}$ and $E^+_{ws,s}$ at small-scale are shown in green in figures 4 and 5. Both cross-correlation functions are shifted slightly to the left, implying that pressure transport occurs just before the energy of 'wavy' streaks. Both correlation functions are also negative, since pressure transport removes energy from the streamwise component.

Energy Cascade

As seen in figures 2 and 3, the large-scale turbulent transport term T^+_{ul} is mostly negative across the wall-normal domain, while the small-scale term T^+_{us} is mostly positive. In addition, the small-scale dissipation term ε^+_{us} has much greater magnitude than its large-scale counterpart. This is indicative of the transfer of energy from large- to small-scales in the classical energy cascade. To investigate its relation to the self-sustaining process at each scale, the temporal cross correlations of T^+_{uls} and $E^+_{ws,l}$, and ε^+_{us} and $E^+_{wr,s}$ are shown in figure 6, where T^+_{uls} represents the transfer of energy directly from u^+_l to u^+_s. The turbulent transport

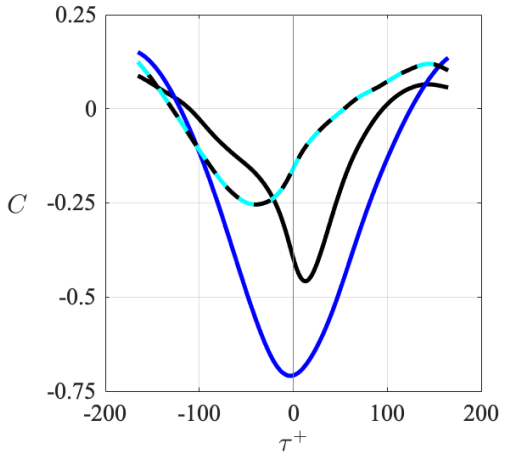

Figure 6. Temporal cross-correlations between T^+_{uls} & $E^+_{ws,l}$ (black), ε^+_{us} & $E^+_{wr,s}$ (blue), and T^+_{uls} & ε^+_{us} (dashed blue/black).

term T^+_{uls} correlates well with $E^+_{ws,l}$ with a right-shifted peak and the dissipation term ε^+_{us} correlates very well with $E^+_{wr,s}$, suggesting that the energy cascade is most active during the late stages of streak breakdown at each scale. Finally, the cross-correlation of T^+_{uls} with ε^+_{us} is also shown, which shows reasonably good agreement and a left-shifted peak at $\tau^+ \approx -40$.

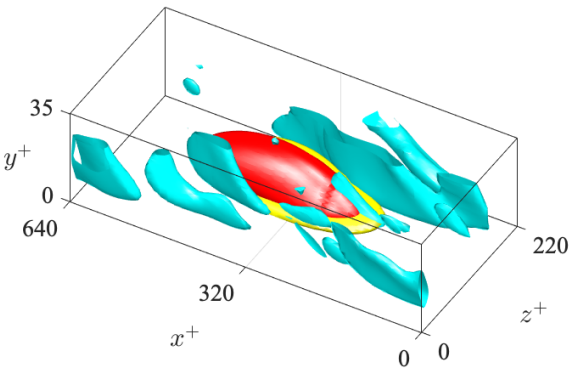

Figure 7. The formation of a large-scale structure by small-scale structures: isosurfaces of u^+_l (red), u^+_s (blue) and $T^+_{in,ul}$ (yellow).

Energy Transfer from Small to Large Scales

In order to study the temporal dynamics of small- to large-scale energy transfer, the time series of $T^+_{in,ul}$ is analysed and local maximum points are identified. Such an event is shown in figure 7, where positive isosurfaces of $T^+_{in,ul}$ are shown in yellow, u^+_l in red and u^+_s in blue. During the event, the isosurfaces of $T^+_{in,ul}$ form alongside the small-scale streaks and precede the growth of the large-scale streaks and the small-scale streaks subsequently de-

cay. The full dynamics of such scale interaction events will be discussed in the presentation.

CONCLUSIONS

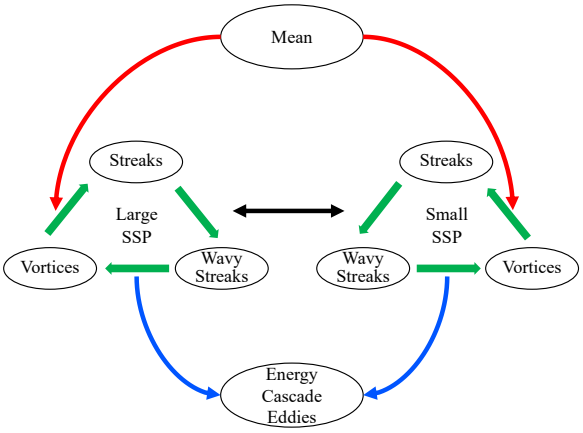

Figure 8. Schematic diagram of the two-scale system.

In this work, the temporal dynamics of a near-wall flow with two integral lengthscales of motion are analysed. The turbulent production terms, which fuel the self-sustaining process at each scale, are correlated with the lift-up effect, while the pressure transport terms are correlated with streak instability. The cascade of energy from large- to small-scales is most active during the late stages of streak breakdown at both large- and small-scales, as seen through the cross-correlations of inter-scale turbulent transport and small-scale dissipation. Finally, highly intermittent small- to large-scale energy transfer events are identified, which result in the formation of wall-parallel large-scale structures.

REFERENCES

Agostini, Lionel & Leschziner, Michael 2016 Predicting the response of small-scale near-wall turbulence to large-scale outer motions. *Physics of Fluids* **28** (1), 015107.

Cho, Minjeong, Hwang, Yongyun & Choi, Haecheon 2018 Scale interactions and spectral energy transfer in turbulent channel flow. *Journal of Fluid Mechanics* **854**, 474–504.

Doohan, Patrick, Willis, Ashley P. & Hwang, Yongyun 2019 Shear stress-driven flow: the state space of near-wall turbulence as $re_\tau \to \infty$. Submitted.

de Giovanetti, Matteo, Hwang, Yongyun & Choi, Haecheon 2016 Skin-friction generation by attached eddies in turbulent channel flow. *Journal of Fluid Mechanics* **808**, 511–538.

Hamilton, James M, Kim, John & Waleffe, Fabian 1995 Regeneration mechanisms of near-wall turbulence structures. *Journal of Fluid Mechanics* **287**, 317–348.

Hwang, Yongyun 2015 Statistical structure of self-sustaining attached eddies in turbulent channel flow. *Journal of Fluid Mechanics* **767**, 254–289.

Hwang, Yongyun 2016 Mesolayer of attached eddies in turbulent channel flow. *Physical Review Fluids* **1** (6), 064401.

Hwang, Yongyun & Bengana, Yacine 2016 Self-sustaining process of minimal attached eddies in turbulent channel flow. *Journal of Fluid Mechanics* **795**, 708–738.

Hwang, Yongyun & Cossu, Carlo 2010 Self-sustained process at large scales in turbulent channel flow. *Physical review letters* **105** (4), 044505.

Hwang, Yongyun & Cossu, Carlo 2011 Self-sustained processes in the logarithmic layer of turbulent channel flows. *Physics of Fluids* **23** (6), 061702.

Jiménez, Javier & Moin, Parviz 1991 The minimal flow unit in near-wall turbulence. *Journal of Fluid Mechanics* **225**, 213–240.

Jiménez, Javier & Pinelli, Alfredo 1999 The autonomous cycle of near-wall turbulence. *Journal of Fluid Mechanics* **389**, 335–359.

Kolmogorov, Andrey Nikolaevich 1941 The local structure of turbulence in incompressible viscous fluid for very large reynolds numbers. In *Dokl. Akad. Nauk SSSR*, , vol. 30, pp. 299–303.

Kolmogorov, Andrei Nikolaevich 1991 The local structure of turbulence in incompressible viscous fluid for very large reynolds numbers. *Proc. R. Soc. Lond. A* **434** (1890), 9–13.

Lee, Myoungkyu & Moser, Robert D 2015 Spectral analysis on reynolds stress transport equation in high re wall-bounded turbulence. In *TSFP DIGITAL LIBRARY ONLINE*. Begel House Inc.

Long, Robert R & Chen, Tien-Chay 1981 Experimental evidence for the existence of the 'mesolayer'in turbulent systems. *Journal of Fluid Mechanics* **105**, 19–59.

Marusic, Ivan, Monty, Jason P, Hultmark, Marcus & Smits, Alexander J 2013 On the logarithmic region in wall turbulence. *Journal of Fluid Mechanics* **716**.

Mathis, Romain, Hutchins, Nicholas & Marusic, Ivan 2009 Large-scale amplitude modulation of the small-scale structures in turbulent boundary layers. *Journal of Fluid Mechanics* **628**, 311–337.

Sreenivasan, Katepalli R & Sahay, Anupam 1997 The persistence of viscous effects in the overlap region, and the mean velocity in turbulent pipe and channel flows. In *Self-Sustaining Mechanisms of Wall Turbulence* (ed. Ronald Panton), pp. 253–272. Southampton, UK: Computational Mechanics Publications.

Tomkins, Christopher D & Adrian, Ronald J 2003 Spanwise structure and scale growth in turbulent boundary layers. *Journal of Fluid Mechanics* **490**, 37–74.

Townsend, Albert A 1980 *The structure of turbulent shear flow*. Cambridge university press.

Wei, T, Fife, P, Klewicki, J & McMurtry, P 2005 Properties of the mean momentum balance in turbulent boundary layer, pipe and channel flows. *Journal of Fluid Mechanics* **522**, 303–327.